

Topological Morphology of Methylsilsesquioxane Derivatives

Ippei Noda,* Takeshi Kamoto, Yosuke Sasaki, and Masahiko Yamada

Research and Development Division, Takemoto Oil and Fat Company, Limited,
2-5 Minato-machi, Gamagori, Aichi 443-8611, Japan

Received August 18, 1999. Revised Manuscript Received September 27, 1999

A change in the morphological topology of particles of methylsilsesquioxane derivatives is observed with a change in the silicone monomer formulation. The particles change from a spherical shape to a hollow hemispherical shape with an increase in the content of silica-forming monomers in methylsilsesquioxane-forming monomers, whereas the spherical shape does not change with the addition of dimethyl silicone-forming monomers to methylsilsesquioxane-forming monomers. The intermediate shape is a sphere surrounded by a wrinkly surface, like a soccer ball, and the particle finally becomes a hollow hemisphere. These phenomena were examined by FT-IR, ^{29}Si CP/MAS NMR (solid-state), and XPS spectra from the perspective of internal steric stress due to tetra- or trifunctional units in the particle core.

1. Introduction

Polymeric siloxanes are of considerable interest because of their promising bulk properties, including thermal stability.¹ Amorphous polymeric siloxanes with unique properties are optically transparent between 250 and 600 nm and are comparable to silica glasses.^{1c,2} Recently, there has been increasing interest in controlling micro- and nanostructured materials, for example microtubes and nanotubes, to produce amorphous optical materials with low light-scattering loss and small double-refraction.³ Sol-gel methods and emulsion polymerization, which can easily produce a three-dimensional inorganic network by chemical reaction at relatively low temperature, are attractive due to their potential application in the preparation of these target materials.^{4,5} As part of an effort to obtain a suitable particle shape for industrial needs, spherical particles of methylsilsesquioxane have been used to improve the lubrication properties of polyester films.⁶ In particular, methylsilsesquioxane particles are widely used in thin

polyester films for magnetic media, whereas these particles are not useful in transparent wrapping films because they become cloudy. Wrapping films are typically thicker than magnetic films, and these transparent films are posttreated by high-speed printing and/or coating. The friction properties of thick films only improve with the addition of larger particles. On the other hand, these particles cause cloudiness of the films due to the particle size. The degree of transparency of such films as estimated by a haze value⁷ is affected by the difference in the refractive index between the particles and film, the particle size, and the concentration of additive particles. The transparency of film should be maintained if the difference in the refractive index between the polyester and particles is within 0.03⁸ or if the particles are smaller than 0.4 μm .⁹

Therefore, it is possible that the lubricity of a transparent polyester film may be improved by the addition of particles with a hollow hemisphere shape, whose thickness is under 0.4 μm . In addition, a small amount of the hemispherical particle is capable of producing the same surface roughness of the film relative to spherical particle, since the shape of the protrusions is not sharp. Consequently, the haze is not relatively influenced by bulk scattering caused by particles within the matrix.

The preparation of a spherical forms of methylsilsesquioxane from methyltrialkoxysilanes^{6,10} and silica

(1) (a) Rochow, E. G. *Silicon and Silicones*; Springer-Verlag: Berlin, 1987. (b) Stark, F. O.; Falander, J. R.; Wright, A. P. *Comprehensive Organic Chemistry*; Wilkinson, G., Stone, F. G. A., Eds.; Pergamon Press: London, 1982; pp 305–364. (c) Baney, R. H.; Ito, M.; Sakakibara, A.; T. Suzuki, T. *Chem. Rev.* **1995**, *95*, 1409.

(2) (a) Brown, J. F., Jr.; Vogt, L. H., Jr.; Katchman, A.; Eutance, J. W.; Kiser, K. M.; Krantz, K. W. *J. Am. Chem. Soc.* **1960**, *82*, 6194. (b) Matsui, F. *Kobunshi Kakou* **1990**, *39*, 299.

(3) (a) Ishigure, T.; Nihei, E.; Koike, Y. *Appl. Opt.* **1994**, *33*, 4261. (b) Kurokawa, T.; Takano, N.; Oikawa, S.; Okada, T. *Appl. Opt.* **1978**, *17*, 646. (c) Prasad, P. N.; Williams, D. J. *Introduction to Nonlinear Optical Effects in Molecules and Polymers*; John Wiley & Sons: New York, 1990. (d) Usui, M.; Hikata, M.; Watanabe, T.; Amano, M.; Sugawara, S.; Hayashida, S.; Imamura, S. *IEEE J. Lightwave Technol.* **1996**, *14*, 2338. (e) Kaino, T. *J. Polym. Sci. Part A* **1987**, *25*, 37. (f) Imamura, S.; Yoshimura, R.; Izawa, T. *Electron. Lett.* **1991**, *27*, 1342. (g) Martin, C. R. *Science* **1994**, *266*, 1961. (h) Martin, C. R. *Acc. Chem. Res.* **1995**, *28*, 61.

(4) (a) Brinker, C. J.; Scherer, G. W. *Sol-Gel Science*; Academic Press: New York, 1990. (b) Iler, R. K. *The Chemistry of Silica*; John Wiley and Sons: New York, 1979.

(5) Baumann, F.; Schmid, M.; Deubzer, B.; Geck, M.; Dauth, J. *Macromolecules* **1994**, *27*, 6102.

(6) Noda, I.; Isikawa, M.; Yamawaki, M.; Sasaki, Y. *Inorg. Chim. Acta* **1997**, *263*, 149.

(7) ASTM Designation D-1003–52, in part 27, *Annual Book of ASTM Standards*; ASTM: Philadelphia, PA, 1974.

(8) Krevelen, V. *Properties of Polymers*; Elsevier: Amsterdam, 1976.

(9) Lipko, J. D.; George, H. F.; Thomas, D. A.; Hargest, S. C.; Sperling, L. H. *J. Appl. Polym. Sci.* **1979**, *23*, 183.

(10) See for example: (a) Kimura, H. Japanese Patent Kokai-S-63-77940, 1988; *Chem. Abstr.* **1988**, *109*, 74167. (b) Kimura, H.; Takahashi, T. Japanese Patent Kokai-S-63-295637, 1988; *Chem. Abstr.* **1989**, *110*, 174011. (c) Nishida, M.; Takahashi, T.; Kimura, H. Japanese Patent Kokai-H-1-242625, 1989; *Chem. Abstr.* **1990**, *112*, 99962. (d) Terae, N.; Iguchi, Y.; Okamoto, T.; Sudo, M. Japanese Patent Kokai-H-2-209927, 1990; *Chem. Abstr.* **1991**, *114*, 43819.

from tetraalkoxysilane¹¹ has been reported, whereas particles with nonspherical shapes were not obtained by polymerization from these monomers in aqueous solution. In the course of our studies on the synthesis of uniform particles, several topological morphologies of particles were observed with a change in the silicone monomer composition, and the resulting compounds were suitable for use as lubricating particles in a transparent polyester film.

In this paper, we describe a method for preparing methylsilsesquioxane derivatives of a suitable particle shape by emulsion polymerization.

2. Experimental Section

2.1. General Data. The scanning electron microscopy micrographs were taken using a JEOL JSM-T300 microscope. The IR spectra were measured by a HORIBA FT-IR spectrometer. Attenuated total reflectance infrared (ATR IR) spectra were obtained using a HORIBA FT-IR spectrometer with a germanium internal reflection element. The ²⁹Si CP/MAS NMR spectra were recorded on a JEOL LA-400 with tetramethylsilane used as an external standard. The median diameter of particles were measured on a HORIBA CAPA-700 centrifuge sedimentation particle size distributor and a HORIBA LA-700 laser scattering particle size distributor. The X-ray photoelectron spectroscopy (XPS) spectra were recorded using a SHIMADZU ESCA 850 spectrometer with Mg K α excitation at 90° takeoff angle.

2.2. General Method. 2.2.1. Average Diameter and Standard Deviation of Particle Size. Particles were photographed using a JEOL scanning electron microscope JSM-T300, and 50 particles were arbitrarily selected by the photographic image. The average diameter of the selected spherical particles was measured from the photographs, whereas the average major and minor axes of the selected hemispherical particles were calculated respectively from the photographs. The standard deviation of the particle size was estimated from the diameter or the major and minor axes of each particle.

2.2.2. Media Diameter and Distribution of Particle Size Measured by CAPA-700. The particles were dispersed by water containing 5 wt % of 10 mol adduct of nonylphenol ethylene oxide by use of ultrasonic waves. The following measurements were taken by using such dispersions by means of CAPA-700, and the density of each particle was calculated with an interpolation between methylsilsesquioxane and silica.

2.3. Materials. Methyltrimethoxysilane, ethylsilicate, dimethyldimethoxysilane, and sodium dodecylbenzenesulfonic acid were commercial grades and used without further purification.

Preparation of Silicone Polymer Particle 2 (as a Typical Procedure) Described in Detail. A mixture of methyltrimethoxysilane (117.0 g, 0.86 mol) and tetraethoxysilane (19.9 g, 0.096 mol) was added dropwise into pure water (831.6 mL) and 48% sodium hydroxide (0.65 g) over a period of 20 min, maintaining the two layers. The mixture was slowly stirred at 14 °C. After 50 min, 5% sodium dodecylbenzenesulfonic acid (6.0 g) was added dropwise into reaction mixture. After aging for 10 h, separation of resulting precipitates by centrifugation, washing with pure water (200 mL), and drying for 12 h under reduced pressure (90 °C/1 Torr) afforded 49.2 g (76%) of silicone particle **2**, empirical formula $\{(\text{CH}_3)_{0.9}\text{SiO}_{1.55}\}$, as a white powder: ²⁹Si CP/MAS NMR (solid state) δ -65.7 $\{(\text{CH}_3)\text{Si}^*\text{O}_{3/2}\}$, -56.5 $\{(\text{CH}_3)\text{Si}^*(\text{OH})\text{O}_{2/2}\}$, -109.6 $\{\text{Si}^*\text{O}_{4/2}\}$, -100.3 $\{(\text{HO})\text{Si}^*\text{O}_{3/2}\}$; IR (KBr disk) 3480, 2980, 1640, 1410, 1270, 1130–1030, 830, 780 cm⁻¹; median diameter (LA-700) 2.15 μm ; median diameter (CAPA-700) 2.20 μm .

Silicon Polymer Particle (3). In a manner similar to the preparation of particle **2**, methyltrimethoxysilane (104.2 g, 0.76 mol) and tetraethoxysilane (39.6 g, 0.19 mol) treated with 48% sodium hydroxide (0.5 g) and 5% sodium dodecylbenzenesulfonic acid (6.0 g) gave 47.1 g (74%) of silicone particle **3**, empirical formula $\{(\text{CH}_3)_{0.8}\text{SiO}_{1.60}\}$, as a white powder: ²⁹Si CP/MAS NMR (solid state) δ -65.7 $\{(\text{CH}_3)\text{Si}^*\text{O}_{3/2}\}$, -56.5 $\{(\text{CH}_3)\text{Si}^*(\text{OH})\text{O}_{2/2}\}$, -109.6 $\{\text{Si}^*\text{O}_{4/2}\}$, -100.3 $\{(\text{HO})\text{Si}^*\text{O}_{3/2}\}$; IR (KBr disk) 3480, 2980, 1640, 1410, 1270, 1130–1030, 910, 780 cm⁻¹; median diameter (LA-700) 2.14 μm ; median diameter (CAPA-700) 2.05 μm .

Silicon Polymer Particle (4). In a manner similar to the preparation of particle **2**, methyltrimethoxysilane (91.2 g, 0.67 mol) and tetraethoxysilane (59.8 g, 0.29 mol) treated with 48% sodium hydroxide (0.45 g) and 5% sodium dodecylbenzenesulfonic acid (6.0 g) gave 45.7 g (72%) of silicone particle **4**, empirical formula $\{(\text{CH}_3)_{0.7}\text{SiO}_{1.65}\}$, as a white powder: ²⁹Si CP/MAS NMR (solid state) δ -65.7 $\{(\text{CH}_3)\text{Si}^*\text{O}_{3/2}\}$, -56.5 $\{(\text{CH}_3)\text{Si}^*(\text{OH})\text{O}_{2/2}\}$, -109.6 $\{\text{Si}^*\text{O}_{4/2}\}$, -100.3 $\{(\text{HO})\text{Si}^*\text{O}_{3/2}\}$; IR (KBr disk) 3480, 2980, 1640, 1410, 1270, 1130–1030, 910, 780 cm⁻¹; median diameter (LA-700) 2.13 μm ; median diameter (CAPA-700) 1.72 μm .

Silicon Polymer Particle (5). In a manner similar to the preparation of particle **2**, methyltrimethoxysilane (78.1 g, 0.57 mol) and tetraethoxysilane (79.2 g, 0.38 mol) treated with 48% sodium hydroxide (0.4 g) and 5% sodium dodecylbenzenesulfonic acid (6.0 g) gave 44.5 g (72%) of silicone particle **5**, empirical formula $\{(\text{CH}_3)_{0.6}\text{SiO}_{1.70}\}$, as a white powder: ²⁹Si CP/MAS NMR (solid state) δ -65.7 $\{(\text{CH}_3)\text{Si}^*\text{O}_{3/2}\}$, -56.5 $\{(\text{CH}_3)\text{Si}^*(\text{OH})\text{O}_{2/2}\}$, -109.6 $\{\text{Si}^*\text{O}_{4/2}\}$, -100.3 $\{(\text{HO})\text{Si}^*\text{O}_{3/2}\}$; IR (KBr disk) 3480, 2980, 1640, 1410, 1270, 1130–1030, 910, 780 cm⁻¹; median diameter (LA-700) 2.26 μm ; median diameter (CAPA-700) 1.44 μm .

Silicon Polymer Particle (6). In a manner similar to the preparation of particle **2**, methyltrimethoxysilane (65.1 g, 0.48 mol) and tetraethoxysilane (100.0 g, 0.48 mol) treated with 48% sodium hydroxide (0.3 g) and 5% sodium dodecylbenzenesulfonic acid (6.0 g) gave 41.2 g (67%) of silicone particle **6**, empirical formula $\{(\text{CH}_3)_{0.5}\text{SiO}_{1.75}\}$, as a white powder: ²⁹Si CP/MAS NMR (solid state) δ -65.7 $\{(\text{CH}_3)\text{Si}^*\text{O}_{3/2}\}$, -56.5 $\{(\text{CH}_3)\text{Si}^*(\text{OH})\text{O}_{2/2}\}$, -109.6 $\{\text{Si}^*\text{O}_{4/2}\}$, -100.3 $\{(\text{HO})\text{Si}^*\text{O}_{3/2}\}$; IR (KBr disk) 3480, 2980, 1410, 1270, 1130–1030, 910, 780 cm⁻¹; median diameter (LA-700) 2.20 μm ; median diameter (CAPA-700) 1.27 μm .

Silicon Polymer Particle (7). In a manner similar to the preparation of particle **2**, methyltrimethoxysilane (123.5 g, 0.91 mol) and dimethyldimethoxysilane (12.2 g, 0.10 mol) treated with 48% sodium hydroxide (0.5 g) and 5% sodium dodecylbenzenesulfonic acid (6.0 g) gave 53.2 g (77%) of silicone particle **7**, empirical formula $\{(\text{CH}_3)_{1.1}\text{SiO}_{1.45}\}$, as a white powder: ²⁹Si CP/MAS NMR (solid state) δ -65.7 $\{(\text{CH}_3)\text{Si}^*\text{O}_{3/2}\}$, -56.5 $\{(\text{CH}_3)\text{Si}^*(\text{OH})\text{O}_{2/2}\}$, -19.6 $\{(\text{CH}_3)_2\text{Si}^*\text{O}_{2/2}\}$; IR (KBr disk) 3480, 2980, 1640, 1270, 1130–1030, 910, 850, 780 cm⁻¹; median diameter (LA-700) 2.10 μm ; median diameter (CAPA-700) 2.33 μm .

Silicon Polymer Particle (8). In a manner similar to the preparation of particle **2**, methyltrimethoxysilane (109.8 g, 0.806 mol) and dimethyldimethoxysilane (24.4 g, 0.20 mol) treated with 48% sodium hydroxide (0.7 g) and 5% sodium dodecylbenzenesulfonic acid (6.0 g) gave 51.2 g (73%) of silicone particle **8**, empirical formula $\{(\text{CH}_3)_{1.2}\text{SiO}_{1.40}\}$, as a white powder: ²⁹Si CP/MAS NMR (solid state) δ -65.7 $\{(\text{CH}_3)\text{Si}^*\text{O}_{3/2}\}$, -56.5 $\{(\text{CH}_3)\text{Si}^*(\text{OH})\text{O}_{2/2}\}$, -19.6 $\{(\text{CH}_3)_2\text{Si}^*\text{O}_{2/2}\}$; IR (KBr disk) 3480, 2980, 1640, 1270, 1130–1030, 910, 850, 780 cm⁻¹; median diameter (LA-700) 2.15 μm ; median diameter (CAPA-700) 2.34 μm .

Silicon Polymer Particle (9). In a manner similar to the preparation of particle **2**, methyltrimethoxysilane (67.1 g, 0.49 mol) and dimethyldimethoxysilane (39.5 g, 0.326 mol) treated with 48% sodium hydroxide (0.5 g) and 5% sodium dodecylbenzenesulfonic acid (6.0 g) gave 45.7 g (76%) of silicone particle **9**, empirical formula $\{(\text{CH}_3)_{1.4}\text{SiO}_{1.30}\}$, as a white powder: ²⁹Si CP/MAS NMR (solid state) δ -65.7 $\{(\text{CH}_3)\text{Si}^*\text{O}_{3/2}\}$, -56.5 $\{(\text{CH}_3)\text{Si}^*(\text{OH})\text{O}_{2/2}\}$, -19.6 $\{(\text{CH}_3)_2\text{Si}^*\text{O}_{2/2}\}$; IR (KBr disk) 3480,

(11) Stober, W.; Fink, A.; Bohn, E. *J. Colloid Interface Sci.* **1968**, *26*, 62.

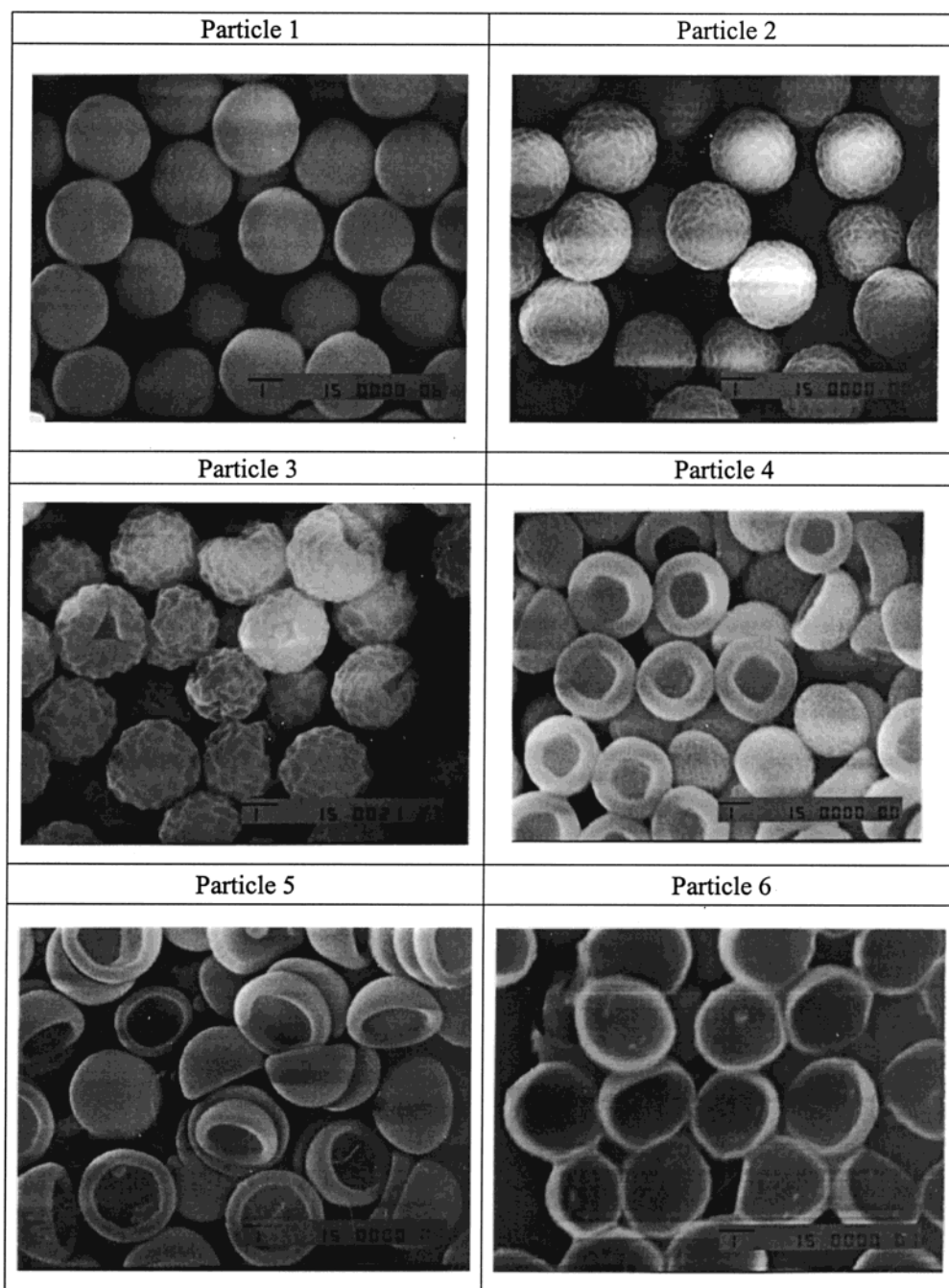


Figure 1. Photographic images of the prepared particles, particles 1–6, by a scanning electron microscope enlarged $\times 10\,000$ times. The maker bar is $1\ \mu\text{m}$.

2980, 1640, 1270, 1130–1030, 910, 850, 780 cm^{-1} ; median diameter (LA-700) $2.11\ \mu\text{m}$; median diameter (CAPA-700) $1.94\ \mu\text{m}$.

3. Results and Discussion

Particles assembled by the polymerization of alkyl-trialkoxysilanes, tetraalkoxysilanes, and dialkyldialkoxysilanes using sodium hydroxide as a catalyst show several exotic topological morphologies caused by topological metamorphosis, as summarized in Figure 1.

These particles are three-dimensional network structures that are distinguished from spherical methylsil-sesquioxane particles by the incorporation of tetra- or difunction fragments as an integral component of the network.

Particles obtained by the polymerization of methyl-trimethoxysilane and a small amount of ethylsilicate were spherically shaped with a wrinkly surface, like a soccer ball. The soccer ball shape is metastable, and particles that assemble by polymerization from silicone monomer with increasing ethylsilicate show a collapse of the wrinkles on their surfaces with some shape transformation. Finally, the particles assume a hollow hemisphere shape, and the thickness of the wall of the bowl decreases as the amount of ethylsilicate in the silicone monomers increases.

Other particles obtained by the polymerization of methyltrimethoxysilane and dimethyldimethoxysilane do not undergo topological metamorphosis of the particle shape. As the dimethyldimethoxysilane content in-

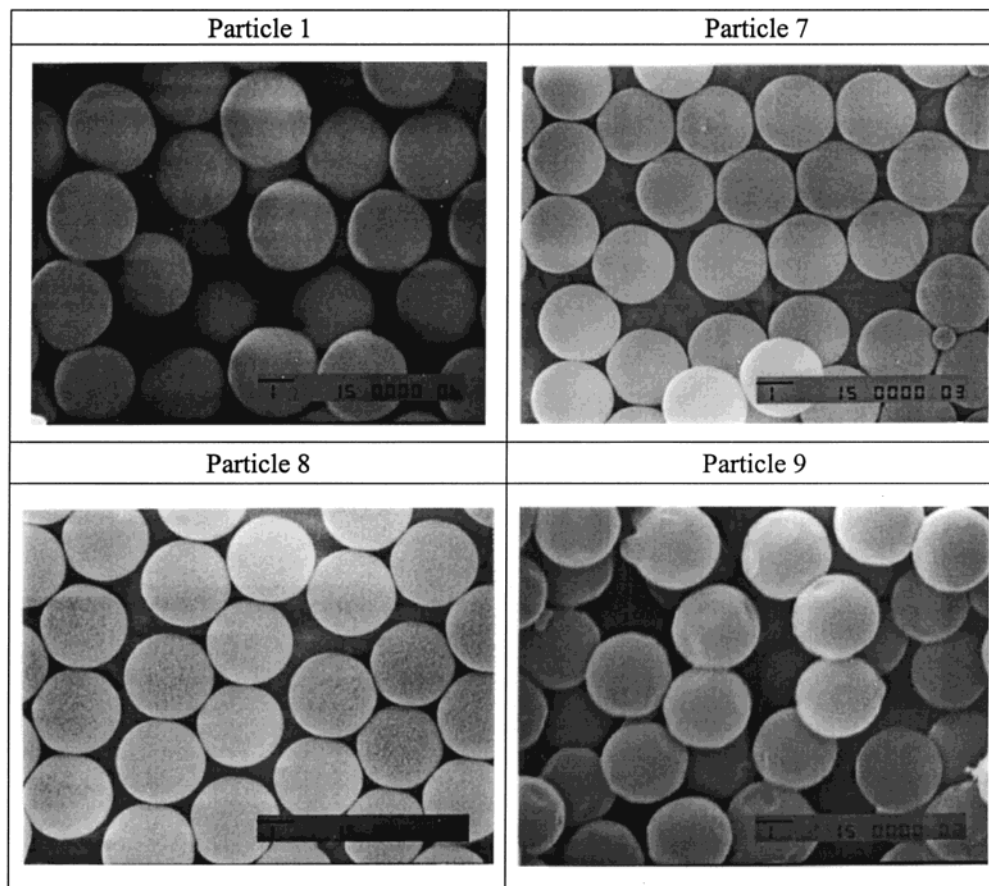


Figure 2. Photographic images of the prepared particles, particles 1, 7, 8, and 9, by a scanning electron microscope. All photographs enlarged $\times 10\,000$ times. The maker bar is $1\ \mu\text{m}$.

creases, the surface of the particles becomes smoother, as shown in Figure 2.

The Si–O stretching frequencies of these particle absorb in the region $1200\text{--}1000\ \text{cm}^{-1}$.¹² The Si–O stretching vibrations of particles 1, 7, 8, and 9, which contain dimethylsilicone and methylsilicone units, show two strong bands at around 1130 and $1030\ \text{cm}^{-1}$, whereas the absorption of particles 2–6, consisting of methyl silicone and silica units, shows a broad band at around $1080\ \text{cm}^{-1}$ superimposed upon two bands at 1130 and $1030\ \text{cm}^{-1}$ (Figure 3).¹³ The intensity of the band at $1080\ \text{cm}^{-1}$ relative to other bands depends on the content of the silica unit. The Si–CH₃ group displays three characteristic bands near 1410 , 1270 , and $780\ \text{cm}^{-1}$.^{12a}

The chemical shifts of silicon in these solid particles were measured by ²⁹Si CP/MAS NMR spectrometry. Two strong peaks at about -65.7 and -56.4 ppm relative to TMS observed with a solid methylsilsesquioxane particle were assigned to each Si atom of (CH₃)SiO_{3/2} and (CH₃)Si(OH)O_{2/2} units.¹⁴ The relative

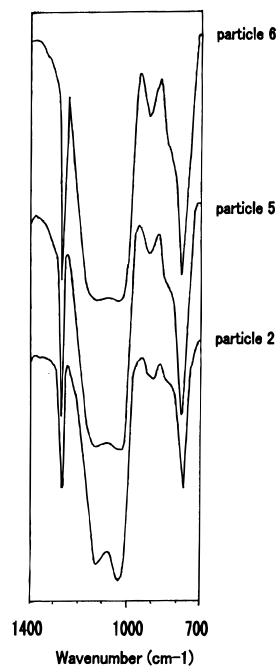


Figure 3. FT-IR spectra of particles 6, 5, and 2.

intensity of the two peaks is about 2 to 1, and the strongest peak is due to (CH₃)SiO_{3/2}. Particles 7, 8, and 9 show three peaks at -65.8 , -56.5 , and -19.6 ppm, which were associated with Si atoms from (CH₃)SiO_{3/2}, (CH₃)Si(OH)O_{2/2}, and (CH₃)₂SiO_{2/2} (Figure 4).^{14b} The intensity of the three peaks depends on the composition of silicone units in each particle.

(12) See for example: (a) Dire, S.; Camprostrini, R.; Ceccato, R. *Chem. Mater.* **1998**, *10*, 268. (b) Zusho, X.; Ziqun, H.; Daorong, D.; Rongben, Z. *Chin. J. Polym. Sci.* **1994**, *7* (2), 183. (c) Suminoe, T.; Matsumura, Y.; Tomomitsu, O. Japanese Patent Kokoku-S-60-17214, 1985; *Chem. Abstr.* **1978**, *89*, 180824. (d) Fukuyama, S.; Yoneda, Y.; Miyagawa, M.; Nishii, K.; Matsuura, A. European Patent 0406911A1, 1985; *Chem. Abstr.* **1986**, *105*, 115551. (e) Nakashima, H. Japanese Patent Kokai-H-3-227321, 1991; *Chem. Abstr.* **1992**, *116*, 60775.

(13) Urban, M. W.; Gaboury, S. R. *Macromolecules* **1989**, *22*, 1486.

(14) (a) Maciel, G. E.; Sullivan, M. J.; Sindorf, D. W. *Macromolecules* **1981**, *14*, 1607. (b) Engelhardt, G.; Jancke, H.; Lippmaa, E.; Samoson, A. *J. Organomet. Chem.* **1981**, *210*, 295.

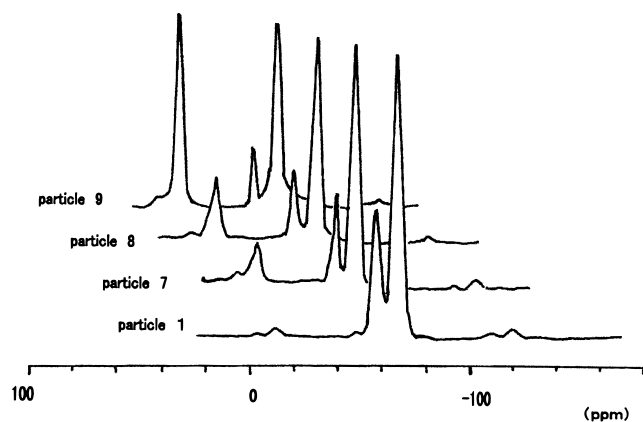


Figure 4. ^{29}Si CP/MAS NMR spectra of solid particles 1, 7, 8, and 9. Chemical shifts are in parts per million from Me_4Si ; large values correspond to lower shielding. Contact time, 10 ms; 4.0-s repetition time.

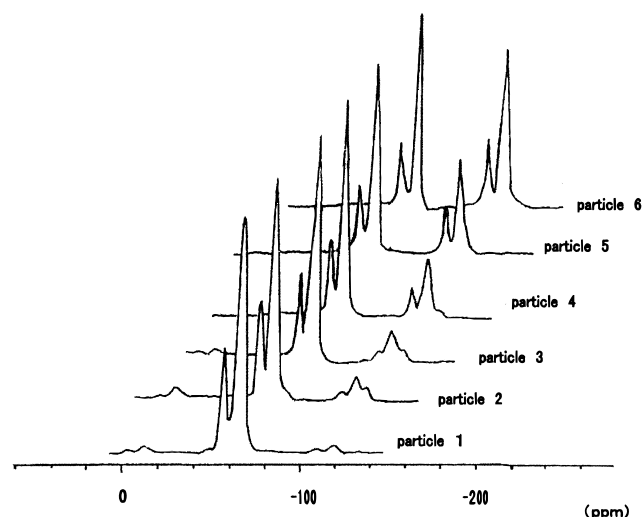


Figure 5. ^{29}Si CP/MAS NMR spectra of solid particles 1, 2, 3, 4, 5, 6. Chemical shifts are in parts per million from Me_4Si ; large values correspond to lower shielding. Contact time, 10 ms; 4.0-s repetition time.

Particles 2–6 characteristically showed four peaks at -65.7 , -56.5 , -109.6 , and -100.3 ppm from $(\text{CH}_3)\text{SiO}_{3/2}$, $(\text{CH}_3)\text{Si}(\text{OH})\text{O}_{2/2}$, $\text{SiO}_{4/2}$, and $(\text{HO})\text{SiO}_{3/2}$, respectively.¹⁵ The intensities of these peaks were proportional to the content of each unit, as shown in Figure 5, however the intensities are not sufficiently quantitative because of side peaks.

These facts indicate that the degree of cross-linking of polymer particles differs with the content of each monomer. The degree of structural freedom relative to the difference in the degree of cross-linking affects the particle shape. Bifunctional units of $(\text{CH}_3)_2\text{SiO}_{2/2}$ and $(\text{CH}_3)\text{Si}(\text{OH})\text{O}_{2/2}$ have the greatest freedom of particle shape. Trifunctional units of $(\text{CH}_3)\text{SiO}_{3/2}$ and $(\text{HO})\text{SiO}_{3/2}$ have more mobility than a tetrafunctional unit of $\text{SiO}_{4/2}$. On the basis of these facts, we postulate that the topological metamorphosis of particle shape must occur

to relieve internal steric stress due to tetra- or trifunctional units in the particle core.

The elemental compositions obtained from elemental analyses of these particles are not sufficiently accurate to warrant postulating empirical formulas.^{14a} Therefore, we speculate that particle 1 cured further at 150°C under vacuum for 24 h, since methylsilsesquioxane additionally releases methane and ethanol from 350°C by decomposition to silica.¹⁶ Unfortunately, the ^{29}Si CP/MAS NMR spectra of the resulting methylsilsesquioxane indicates that the peak of the $(\text{CH}_3)\text{Si}(\text{OH})\text{O}_{2/2}$ unit did not completely disappear, as shown in Figure 6.

The volume described by the concavity in the hemispherical particle can be estimated from the complementary information obtained by a centrifugal sedimentation particle size distributor (CAPA-700), a laser-scattering particle size distributor (LA-700), and a scanning electron microscope (SEM). The average major and minor axes of each particle were calculated from 50 particles arbitrarily selected in photographs obtained by SEM. The median diameter of particles with the same refractive index by a laser-scattering particle size distributor is approximately half of the sum of the major and minor axes, as summarized in Table 1.¹⁷ The average diameter of spherical particles estimated from SEM photographs almost agrees with the median diameter obtained using the laser-scattering particle size distributor. These results suggest that the particles are shaped like hemispheres.

The median diameter and size distribution of each particle obtained from the centrifugal sedimentation particle distributor under the Stokes theorem is almost directly proportional to the weight of the particle. The density of each particle is calculated by interpolation between methylsilsesquioxane and silica. The median diameter of hollow-hemisphere particles is less than that measured with a laser-scattering particle size distributor, which is different from the results with spherical particles. If the hemisphere shape is postulated to be pseudo-spherical, the average volume of the hollow in each particle can be calculated with eq 1.¹⁸

The size distribution of particles 2–6 (Figure 7) is broad compared to those of particles 1, 7, 8, and 9.

We also investigated the driving force that causes this topological metamorphosis in particle shape using the ^{29}Si CP/MAS NMR, XPS, and FT-IR spectra of nine representative silicone polymer particles with different topological morphologies.

Particles 2–6 are self-assembled from $(\text{CH}_3)\text{SiO}_{3/2}$, $(\text{CH}_3)\text{Si}(\text{OH})\text{O}_{2/2}$, $\text{SiO}_{4/2}$, and $(\text{HO})\text{SiO}_{3/2}$ units, based on

(16) (a) Bois, L.; Maquet, J.; Babonneau, F.; Mutin, H.; Bahloul, D. *Chem. Mater.* **1994**, *6*, 796. (b) Belot, V.; Corriu, R. J. P.; Leclercq, D.; Mutin, P. H.; Vioux, A. *J. Polym. Sci., Part A* **1992**, *30*, 613. (c) Kitakohji, T.; Takeda, S.; Nakajima, M.; Usui, M. *Jpn. J. Appl. Phys.* **1983**, *22*, 1934. (d) Nakashima, H. Japanese Patent Kokai-H-3-227321, 1991; *Chem. Abstr.* **1992**, *116*, 60775. (e) Li, D.; Hwang, S. T. *J. Appl. Polym. Sci.* **1992**, *44*, 1979.

(17) (a) Chu, B. *Laser Light Scattering*; Academic: New York, 1974. (b) Chu, B.; Xu, R.; Dinapoli, A. *J. Colloid Interface Sci.* **1987**, *116*, 183.

(18) The average volume of a hollow in half bowl shape particles were calculated with eq 1.

$$\text{hollow volume} = \frac{4}{3} \left(\frac{\gamma_1^3}{8} - \frac{\gamma_2^3}{8} \right) \pi \quad (1)$$

γ_1 : average diameter of particles obtained with a laser scattering particle size distributor. γ_2 : median diameter of particles estimated with a centrifuge sedimentation particle size distributor.

(15) (a) Lippmaa, E. T.; Alla, M.; Pehk, T. J.; Engelhardt, G. *J. Am. Chem. Soc.* **1978**, *100*, 1929. (b) Lippmaa, E.; Magi, M.; Samoson, A.; Engelhardt, G.; Grimmer, A.-R. *J. Am. Chem. Soc.* **1980**, *102*, 4889. (c) Pesek, J. J.; Sandoval, J. E.; Chu, C.-H.; Josseon, E. *Chemically Modified Surfaces*; Mottola, H. A., Steinmetz, J. R., Eds; Elsevier: Amsterdam, 1992; pp 57–72.

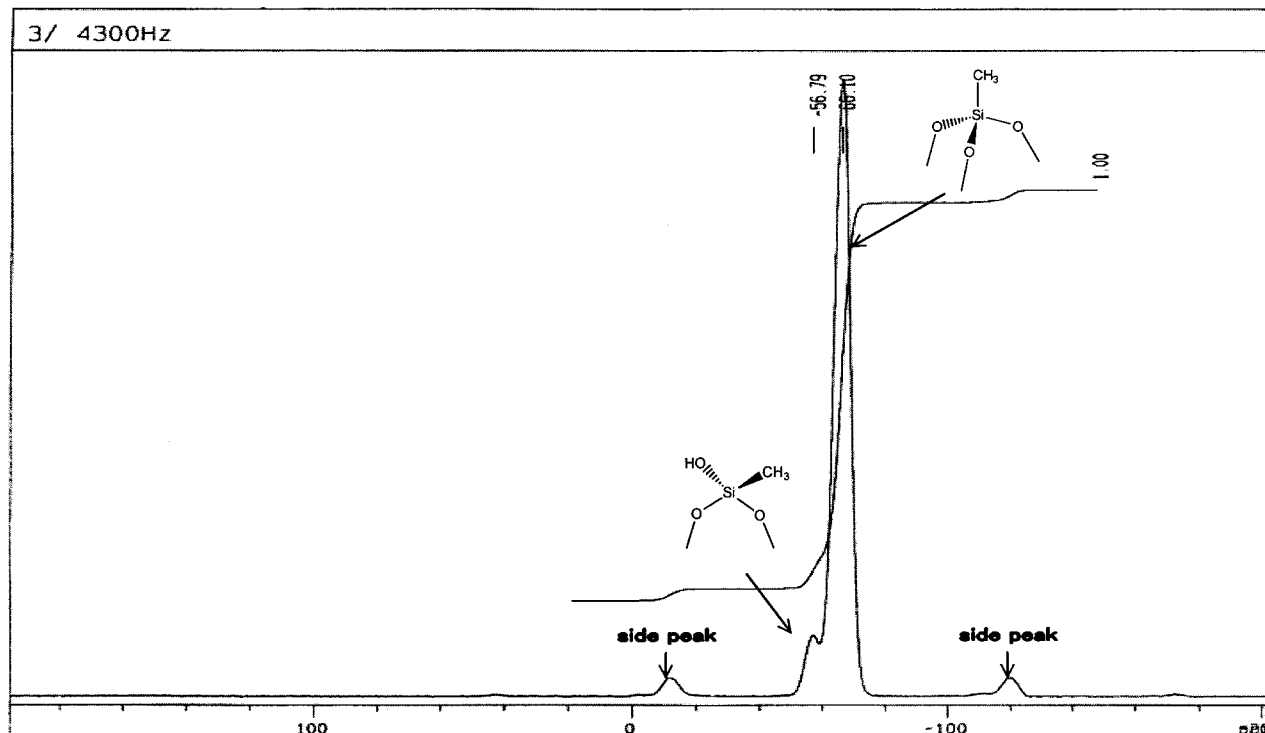


Figure 6. ^{29}Si CP/MAS NMR spectra of solid resulting particle cured still more from particle 4. Chemical shifts are in parts per million from Me_4Si ; large values correspond to lower shielding. Contact time, 10 ms; 4.0-s repetition time.

Table 1. Average Hollow Volume of Particles 3–5 Calculated with Eq 1

particle	SEM technique			median diameter (LA-700) (μm)	median diameter (CAPA-700) (μm)	av hollow vol (μm^3)
	av major axis (μm)	av minor axis (μm)	av thickness (μm)			
3	2.4	1.9	0.84	2.14	2.05	0.62
4	2.4	1.5	0.60	2.13	1.72	2.39
5	2.5	1.7	0.35	2.26	1.44	4.47

^{29}Si CP/MAS NMR spectra. The empirical formula of each particle predicted for a quantitative reaction is comparable to the observed formula estimated from XPS atomic composition data, and the observed formula of particle 2 is $\text{C}_{2.0}\text{SiO}_{2.0}$, which is different from the predicted formula of $\text{C}_{0.9}\text{SiO}_{1.55}$. XPS analysis generally gave the most lucid data for surface analysis, and atomic concentration data indicate the composition of the outer 40 Å.¹⁹ The difference in atomic composition indicates that the outer structure to a depth of about 40 Å is distinguishable from the inner structure. Furthermore, $\text{SiO}_{4/2}$ and $(\text{HO})\text{SiO}_{3/2}$ units exist in the inner part of the particle, relative to $(\text{CH}_3)\text{SiO}_{3/2}$ and $(\text{CH}_3)\text{Si}(\text{OH})\text{O}_{2/2}$ units, based on XPS atomic composition data, since tetraalkoxysilicates are more readily hydrolyzed with a basic catalyst than methyltrialkoxysilanes.²⁰ These facts are supported by a small hydroxyl group value for these particles 1–3, if the hydroxyl group value signifies hydroxyl group particles on the surface.²¹ This spherical shape resulting from the heterogeneous structure obtained by the aqueous self-assembly of tetraethylsilicate

and methyltrimethoxysilane should be the most stable topological morphology against crushing damage due to water pressure. From particle 3 to particle 6, the steric stress in the particle core becomes greater than the external water pressure, and topological metamorphosis occurs due to the relaxation of internal steric stress. Hence, the particles 1–6 change shape from a sphere to a hollow hemisphere with an increase in $\text{SiO}_{4/2}$ and $(\text{HO})\text{SiO}_{3/2}$ units. The observed formulas for particles 3–6 are equal to the predicted empirical formulas, as summarized in Tables 2 and 3. Finally, the observed formula of particle 6 is approximately equal to the predicted formula, since it has the largest surface area, and the large hydroxyl group value of particle 6 is consistent with XPS spectra, which reflect a homogeneous structure. Thus, we postulated that the topological metamorphosis in particle shape from a heterogeneous structure to a homogeneous structure is caused by the relaxation of steric stress of inner $\text{SiO}_{4/2}$ and $(\text{HO})\text{SiO}_{3/2}$ units, which are found predominantly near the core of the particle. On the other hand, particles 7–9 consist of $(\text{CH}_3)\text{SiO}_{3/2}$, $(\text{CH}_3)\text{Si}(\text{OH})\text{O}_{2/2}$, and $(\text{CH}_3)_2\text{SiO}_{2/2}$ units according to ^{29}Si CP/MAS NMR spectra, and these observed formulas are close to the predicted formulas with an increase in $(\text{CH}_3)_2\text{SiO}_{2/2}$ units, as shown in Table 3. $(\text{CH}_3)_2\text{SiO}_{2/2}$ units have structural freedom because they are difunctional, and the internal steric stress due to the difference between the inner and outer structures is relieved by the addition of a $(\text{CH}_3)_2\text{SiO}_{2/2}$ unit. The stable form of particles 7–9 is a spherical shape from the perspective of the internal steric stress in the particle core, and a sphere with more $(\text{CH}_3)_2\text{SiO}_{2/2}$ units than particle 9 should be more stable to maintain a three-dimensional spherical network with a low degree of cross-linking. A reduction in the hydroxyl

(19) Clark, D. T.; Thomas, H. R. *J. Polym. Sci. Polym. Chem. Ed.* **1977**, *15*, 2843.

(20) Kim, J.; Plawsky, J. L.; Wagenen, E. V.; Korenowski, G. M. *Chem. Mater.* **1993**, *5*, 1118.

(21) Rowe, E. L.; Machkoveck, S. M. *J. Pharm. Sci.* **1977**, *66*, 273.

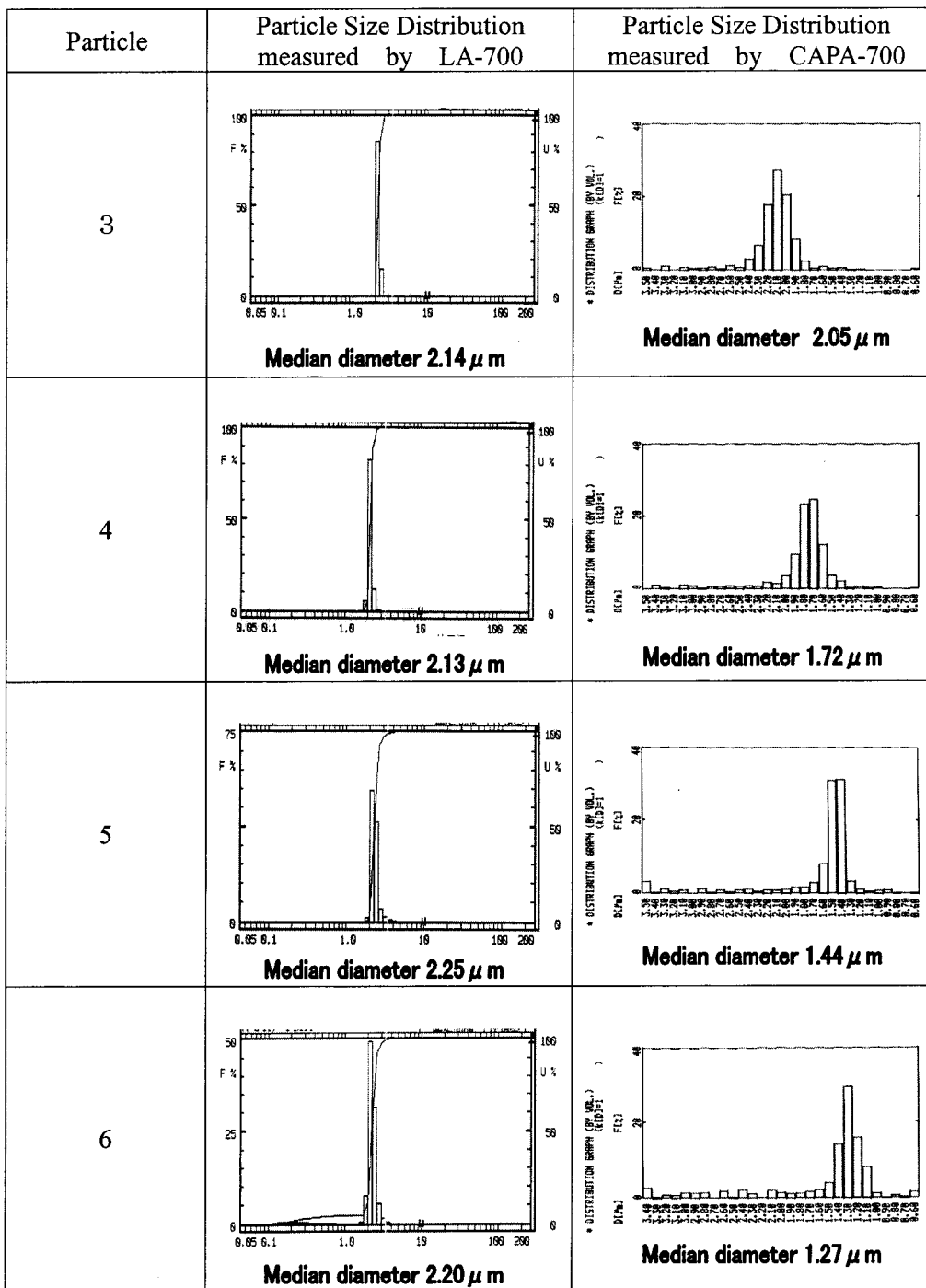


Figure 7. Median diameter and diameter distribution of particles 3–6 measured from LA-700 and CAPA-700.

Table 2. Relationship between Atomic Abundance Measured by ESCA and Hydroxyl Group Value of Each Particle

particle	atomic abundance calculated by ESCA spectra			hydroxyl group value (KOH mg/g)
	carbon	oxygen	silicon	
1	41.1	35.5	23.4	37.6
2	40.4	39.8	19.8	38.1
3	34.5	43.3	22.3	41.5
4	30.4	45.5	24.1	42.2
5	28.7	47.7	23.6	42.8
6	16.2	56.1	27.7	54.5
7	40.5	36.5	23.4	25.3
8	36.1	37.6	26.2	37.3
9	39.4	34.8	25.8	76.7

Table 3. Empirical Formula Predicted for a Quantitative Reaction and Atomic Formula Estimated from XPS Atomic Composition Data (90° Takeoff Angle) for Each Particle

particle	empirical formula	found
1	C _{1.0} SiO _{1.50}	C _{1.8} SiO _{1.5}
2	C _{0.9} SiO _{1.55}	C _{2.0} SiO _{2.0}
3	C _{0.8} SiO _{1.60}	C _{1.5} SiO _{1.9}
4	C _{0.7} SiO _{1.65}	C _{1.3} SiO _{1.9}
5	C _{0.6} SiO _{1.70}	C _{1.2} SiO _{2.0}
6	C _{0.5} SiO _{1.75}	C _{0.6} SiO _{2.0}
7	C _{1.1} SiO _{1.45}	C _{1.7} SiO _{1.6}
8	C _{1.2} SiO _{1.40}	C _{1.4} SiO _{1.4}
9	C _{1.4} SiO _{1.30}	C _{1.5} SiO _{1.3}

group value predicted from the empirical formula of particles 7–9 is not observed, since the hydroxyl value

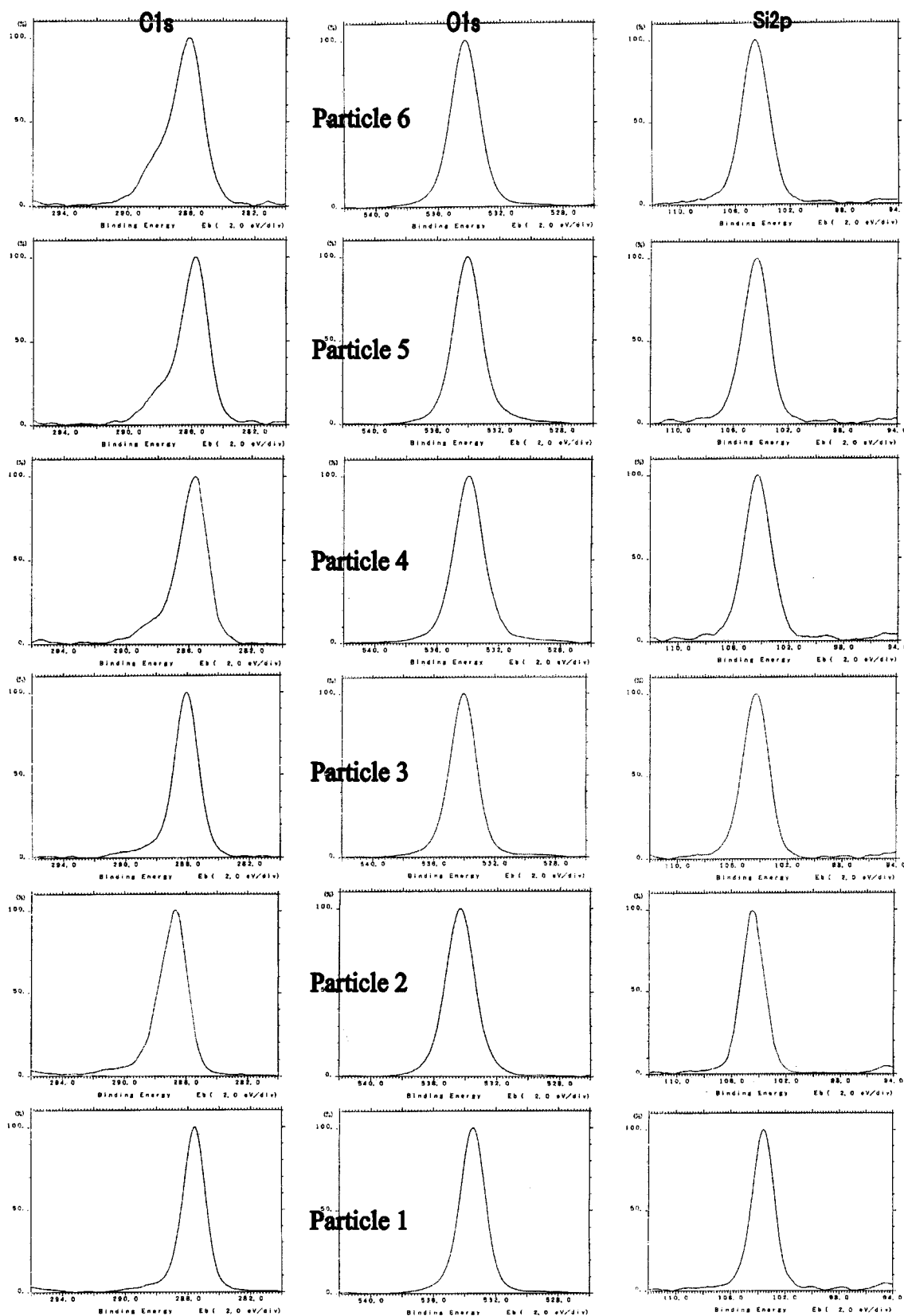


Figure 8. XPS spectra of particles 2–9 containing $\text{SiO}_{4/2}$ and $(\text{HO})\text{SiO}_{3/2}$ segments, which are compared with XPS spectra of particle 1.

probably reflects all of the hydroxyl groups of the particles comprising the low cross-linking network structure, which have a larger pore size and volume.

The atomic abundance estimated from the XPS spectra, hydroxyl group value, empirical formula, and ob-

served formula of each particle is summarized in Tables 2 and 3.

The high binding energy shoulder observed in the C 1s region of particles 3–6 (Figure 8) suggests that the carbon atom of the methyl group interacts with neigh-

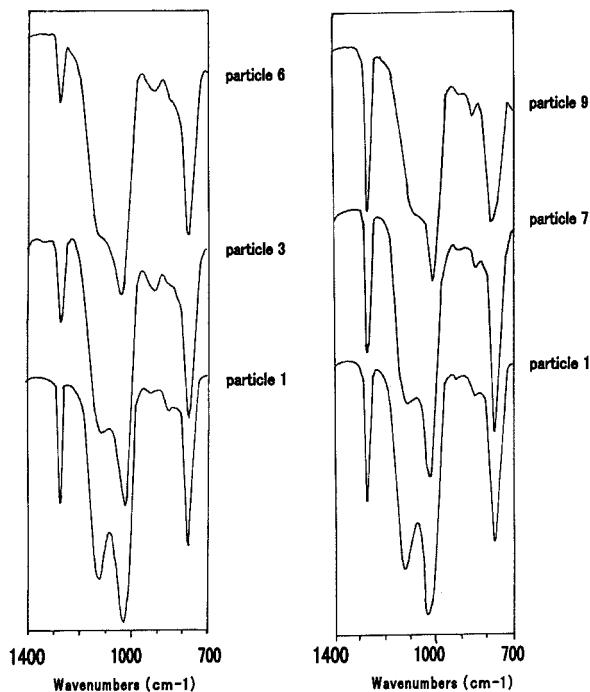


Figure 9. ATR FT-IR spectra of methylsilsesquioxane particles derived by the topological metamorphosis.

boring oxygen atoms. These interactions increase with an increase in $\text{SiO}_{4/2}$ and $(\text{HO})\text{SiO}_{3/2}$ units.

ATR IR spectra of these particles are indistinguishable from their IR spectra (KBr disk method), except for a slight difference in intensities, as shown in Figure 9. The intensity at 1270 cm^{-1} for particles 2–6 decreases with an increase in $\text{SiO}_{4/2}$ and $(\text{HO})\text{SiO}_{3/2}$ units, whereas the intensity observed in particles 7–8 increases with an increase in $(\text{CH}_3)_2\text{SiO}_{2/2}$ units. In most cases, the ATR IR spectra indicate a depth of less than $0.2\text{--}0.5\ \mu\text{m}$ for $4000\text{--}400\text{ cm}^{-1}$, and the changes emphasize particle surface depths from $40\ \text{\AA}$, based on the results of XPS spectra.²²

(22) Harrick, N. J. *Internal Reflection Spectroscopy*; Wiley-Interscience: New York, 1967.

On the basis of these results obtained with XPS and ^{29}Si CP/MAS NMR spectra, we presume that topological metamorphosis is caused by the relaxation of internal steric stress of inner $\text{SiO}_{4/2}$ and $(\text{HO})\text{SiO}_{3/2}$ units with an increase in surface area.

4. Conclusion

The XPS spectra indicate that the observed topological metamorphosis in the particle shape of methylsilsesquioxane derivatives is caused by the relief of internal stress due to $\text{SiO}_{4/2}$ and $(\text{HO})\text{SiO}_{3/2}$ units in the particle core. In all cases, the most stable topological morphology maintains a balance between the internal stress and external water pressure. The sphere shape surrounded by a wrinkly surface, like a soccer ball, is metastable, although it has the greatest internal stress, since the sphere shape is most stable against external water pressure. The spherical shape becomes more stable with an increase in $(\text{CH}_3)_2\text{SiO}_{2/2}$ units, which have a high degree of structural freedom, whereas with an increase in $\text{SiO}_{4/2}$ and $(\text{HO})\text{SiO}_{3/2}$ units, the spherical shape should change due to internal stress. To reduce internal stress in this case, the particle assumes the most stable topological morphology by topological metamorphosis. The resulting particle is in the shape of a hollow hemisphere, with a narrow size distribution. The wall thickness decreases with an increase in $\text{SiO}_{4/2}$ and $(\text{HO})\text{SiO}_{3/2}$ units. To our knowledge, this study is the first to demonstrate that the wall thickness of a hollow hemisphere can be controlled by this self-assembly reaction.

Acknowledgment. We thank Professor Akira Nakamura (Osaka University) for helpful discussions. We are deeply indebted to Professor Richard H. Holm (Harvard University) for helpful suggestions. Thanks are given to Miss Masumi Sasaki for assistance in the experimental work.

CM990536N